Article ID: 1000-324X(2018)10-1141-06 **DOI:** 10.15541/jim20180227

Influence of Film Thickness on the Electrochemical Performance of α-SiO_x Thin-film Anodes

MENG Xiang-Lu[1,2,3], HUO Han-Yu[1,2], GUO Xiang-Xin[1,4], DONG Shao-Ming[1]

(1. State Key Laboratory of High Performance Ceramics and Superfine Microstructure, Shanghai Institute of Ceramics, Chinese Academy of Sciences, Shanghai 200050, China; 2. University of Chinese Academy of Sciences, Beijing 100049, China; 3. College of Material Science and Technology, ShanghaiTech University, Shanghai 201210, China; 4. College of Physics, Qingdao University, Qingdao 266071, China)

Abstract: SiO_x anodes of lithium ion batteries have attracted considerable attention in recent years, due to their cycle stability, large capacity, and feasibility on composition manipulation. Many previous works have focused on clarifying the influences of oxygen contents on SiO_x based anodes. However, the size effect is still far from understanding. Herein, the size effect on electrochemical properties of SiO_x with thin-film type anodes in different thickness was investigated. It is found that the SiO_x electrodes prepared by sputtering is of a Si/O ratio of 0.7 and exhibits the highest initial Coulombic efficiency (ICE) of 71.68% and the highest capacity retention of 92.01% when the film thickness being 450 nm, compared with those in other thickness. The best performance under such intriguing thickness-performance relationship is attributed to the low charge transfer resistance, formation of the reduced SEI layer and good electrode integrity upon cycling, as evidenced by SEM images and EIS collected during cycling. These results indicate that as anodes of LIBs, the SiO_x anodes with controlled size can greatly improve the electrochemical performance.

Key words: SiO_x thin-film anodes; film thickness; cycle stability; capacity; lithium-ion batteries

Recent years have witnessed the growing demand of high performance lithium ion batteries (LIBs) from portable electronics and electric vehicles. The increase in energy density and safety of LIBs has been the primary duty of the battery research community. In terms of novel anode materials, the specific capacity is a critical parameter to be considered. Si as an anode shows the highest theoretical gravimetric capacity of 3579 $mAh \cdot g^{-1}$ ($Li_{15}Si_4$), which is approximately one order of magnitude higher than that of carbonaceous materials (372 $mAh \cdot g^{-1}$), including graphite, pyrolytic carbon and meso-phase pitch[1-3]. In addition, the electrode potential of Si is below 0.5 V (*vs*. Li/Li^+). As the second abundant element on earth, Si is likewise of great advantages in cost and environmental friendliness. However, the application of Si anodes in LIBs is retarded by the huge volume change (around 300%) appeared during lithiation and delithiation processes[4]. The tremendous volume expansion incurs severe internal mechanical stress, which induces particles fracturing, delamination, and then loss of electrical connection. Consequently, the capacity of Si electrode fades sharply after limited cycles[5-7].

The silicon suboxides (SiO_x) as anodes have received much attention recently, owing to its high capacities and enhanced cycle stability[8-15]. The improved cyclability of SiO_x is ascribed to that the introduced oxygen can be lithiated into inert lithium oxide and other lithium silicate compounds, functioning as the elastic buffers to eliminate the huge structure change upon lithiation and delithiation. In previous study, many works focused on discovering the influence of oxygen contents on the electrochemical performance of SiO_x based anode materials[9,12,14-15]. As proven in previous research, the size of Si particles plays a critical role in cycle performance and rate capability. For the SiO_x anode, the size effect has been scarcely discussed, thus calling for the thorough investigation.

In this study, we investigated the size effect of $SiO_{0.7}$ anodes on the performance by using the thin-film type electrodes. With changing the film thickness of $SiO_{0.7}$ anodes, the cycle stability, initial Coulombic efficiency (ICE) and reversible capacity obviously change. The optimized film thickness for SiO_x anode in terms of reversible capacity, ICE and cyclability can be determined.

Received date: 2018-05-17; **Modified date:** 2018-05-24
Foundation item: National Natural Science Foundation of China (51532002, 51771222, 51772314, 51702346); Taishan Scholars Program
Biography: MENG Xiang-Lu (1991−), male, candidate of Master degree. E-mail: xlumeng@163.com
Corresponding author: GUO Xiang-Xin, professor. E-mail: xxguo@mail.sic.ac.cn; DONG Shao-Ming, professor. E-mail: smdong@mail.sic.ac.cn

Such influence is analyzed from the evolution of electrode surface morphology, charge transfer property and physical structure upon long-term cycling.

1 Experimental

1.1 Synthesis of SiO_x film materials

SiO_x thin-film electrodes were prepared by direct current (DC) reactive magnetron sputtering with a n-type monocrystalline Si of a high purity of 99.999% as the target. The samples were deposited simultaneously on both Si wafer for thickness measurement and rough Cu foil with a thickness of 14 μm for morphology and electrochemical measurements. The distance between target and Si/Cu substrates fixed in 10 cm. Both Ar (99.999%) and O_2 (99.999%) were introduced into the chamber after the base pressure below 3.0×10^{-4} Pa. The gas flow rate of Ar was 20 sccm and and O_2 flow rate used here was 0.8 sccm for depositing $SiO_{0.7}$. The SiO_x thin-films were grown at pressure of 0.55 Pa with a constant DC power supply of 30 W under room temperature. The deposition rate was approximately 9 $nm\cdot min^{-1}$. Before film depositing, the Si target was cleaned by a pre-sputtering. The various film thickness was controlled by the deposition time.

1.2 Materials characterization

The surface morphology and film thickness of the pristine α-SiO_x films were examined by field emission scanning electron microscopy (FESEM, Magellan 400). The crystalline phase of α-SiO_x was determined by X-ray diffraction (XRD, Bruker D8 Phaser with Cu K_α radiation, λ = 0.15406 nm) within the range of 10°–60°. The structure of α-SiO_x films were analyzed by Raman spectrum and the chemical state of α-SiO_x films were analyzed using X-ray photoelectron spectroscopy (XPS, ESCAlab 250).

1.3 Cells assembly and electrochemical measurements

The coin cells in type of 2025 were assembled in an Ar-filled glove box with both the O_2 and H_2O contents below 0.1×10^{-6}. Each cell consisted of α-SiO_x film deposited on rough Cu as the working electrode with 0.785 cm^2 surface area, the separator, the electrolyte and lithium foil with a diameter of 10 mm as the counter electrode. The electrolyte was 1 mol/L $LiPF_6$ dissolved in a 1∶1 (*V*/*V*) mixture solvent of ethylene carbonate (EC) and dimethyl carbonate (DMC) with 1wt% vinylene carbonate (VC) additive. Galvanostatic charge/discharge measurements were carried out with a multichannel battery testing system (LAND CT2001A) in the potential range from 0.01 to 1.5 V at different current densities. The cyclic voltammetry (CV) of SiO_x/Li was performed from 0.01 V to 1.5 V at a scan rate of 0.05 $mV\cdot s^{-1}$ by Arbin BT-2000. Electrochemical impedance spectroscopy (EIS) tests were conducted with a frequency range from 0.1 Hz to 10^5 Hz by an electrochemical workstation (Autolab PGSTAT302N). All the electrochemical measurements were performed at 25℃.

2 Results and discussion

2.1 Characterizations of as-deposited SiO_x film electrodes

The morphology and thickness of SiO_x thin films were examined by FESEM. As shown in Fig. 1(a), the surface of pristine SiO_x film appears rough structure with polygonal particles in size of several microns, which depends on the surface morphology of the Cu foil substrate. This morphology is similarly observed in the MnO thin-film anodes deposited on Cu foils, exhibiting a columnar crystal growth mode[16]. Fig. 1(b) shows a cross-sectional SEM image of SiO_x thin film deposited on a Si wafer, which is used for determining the growth rate of SiO_x thin films[17]. It is found that the thickness of SiO_x thin-film deposited for 20 min is 180 nm corresponding to a growth rate of 9 $nm\cdot min^{-1}$. Fig. 1(c) shows the XRD patterns of the as-deposited SiO_x thin films deposited on rough Cu foil. Two broad peaks centered at 2θ values of 18º and 30º were observed. All the diffraction peaks are assigned to the Cu foil[9,16], and no characteristic peaks of crystalline Si and SiO_2 appear. This indicates that the as-deposited SiO_x films are amorphous. This amorphous feature of SiO_x films is consistent with that characterized in previous reports[8-10]. Fig. 1(d) shows the Raman spectra of as-prepared SiO_x films. In the spectral region between 100 cm^{-1} and 700 cm^{-1}, the spectrum mainly comprises of two broad bands at 160 cm^{-1} and 480 cm^{-1}, which corresponds to the characteristic transverse-acoustic (TA) and transverse-optic (TO) phonon modes of amorphous silicon respectively[18-19]. In addition, no peaks at 520 cm^{-1} corresponding to the characteristic crystalline Si are detected in the spectra of α-SiO_x films[20], further confirm the amorphous feature of the as-prepared SiO_x thin films. Fig. 1(e) shows the XPS Si 2p spectra of the as-deposited SiO_x films near-surface depth profile that was obtained after sputtering with Ar^+ ions for 20 s to remove the surface oxygen layer. To determine the precise valance of Si, The peak shape of $Si2p_{3/2}$ spectra were fitted to a superposition of five peaks with an energy difference of 1 eV, corresponding to the different Si oxidation states, namely Si^0, Si^+, Si^{2+}, Si^{3+} and Si^{4+}[11]. In the curve-fitting process, the position

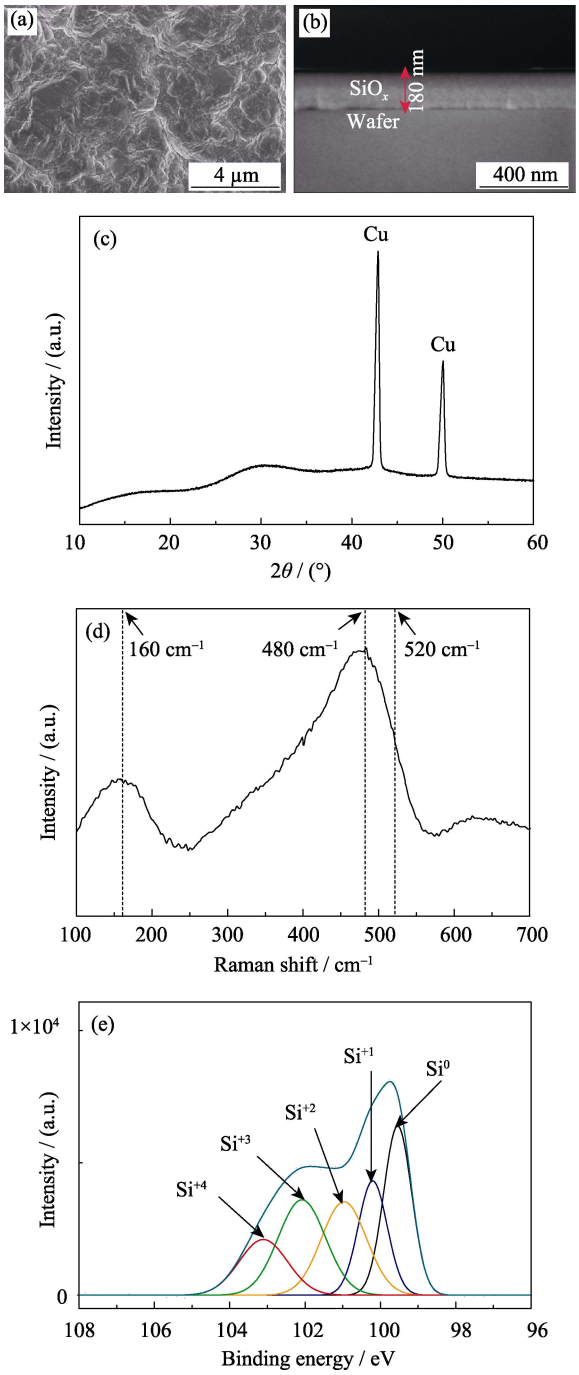

Fig. 1　Characterization of the deposited SiO_x film electrodes. (a) The typical surface morphology of $SiO_{0.7}$ thin film deposited on rough Cu foil; (b) Cross section SEM image of the $SiO_{0.7}$ thin film deposited on Si wafer; (c) XRD patterns of the $SiO_{0.7}$ thin films with a thickness of 450 nm; (d) Raman spectra of as-deposited $SiO_{0.7}$ with a thickness of 450 nm; (e) XPS Si 2p spectral of the $SiO_{0.7}$ thin films with a thickness of 450 nm, which is fitted by using five Si peaks

and full width at half maximum (FWHM) of Si^0 as free parameters were used on the basis of earlier literatures, and the FWHMs of five peaks in each Si2p spectrum show the same value[21-22]. The average valences of Si in the as-prepared SiO_x films can be determined to be 1.4 *via* calculating the deconvoluted peak areas of the five components, corresponding to the chemical formula of $SiO_{0.7}$.

2.2　Effect of film thickness on electrochemical performance of α-SiO_x thin film anodes

It is demonstrated that the $SiO_{0.7}$ anodes possess good cycle performance with reduced capability sacrifice, due to the fact that the moderate oxygen contents enable the formation of sufficient insulated lithium oxide/silicates. This not only relieves the large volume change occurred on *in situ* formed Si particles, but also shields the electrolytes from further decomposition by suppressing electron leakages from electrode surfaces. Therefore, $SiO_{0.7}$ are selected to study the relationship between the film thickness and the electrochemical performance of SiO_x anodes. Coin-type cells with $SiO_{0.7}$ as anodes were assembled and cycled at the current density of 0.064 mA·cm^{-2} (~0.2*C*). Fig. 2 shows the 1st cycle charge-discharge curves of $SiO_{0.7}$ thin-film anodes with the thickness range of 90 nm-630 nm. It is found that the discharge plateaus of all the $SiO_{0.7}$ electrodes with different thickness lie at around 0.23 V, the electrode with different thickness delivers a similar discharge capacity. Upon recharge, the charge plateaus of all the $SiO_{0.7}$ an odes with different thickness lie at the range of 0.2 V-0.75 V. As for the first cycle, the discharge/charge capacities of $SiO_{0.7}$ with thickness of 90 nm, 270 nm, 450 nm and 630 nm are 639.4/410.4, 644.7/443.4, 647.3/464.0 and 641.8/424.9 μAh·cm^{-2}·μm^{-1}, with a corresponding initial Coulombic efficiencies (ICE) of 64.18%, 68.78%, 71.68% and 66.20%, respectively. It is clear that the $SiO_{0.7}$ with a thickness of 450 nm shows the highest ICE. With increasing of film thickness in $SiO_{0.7}$ anodes, the ICE initially increases and then decreases. Formation of solid electrolyte interphase (SEI) is beneficial for shielding the further decomposition of electrolytes on the surface of anodes during discharge but gives rise to extra irreversible capacity, resulting in a low ICE[23]. Beyond the formation of SEI layers, the formation of irreversible

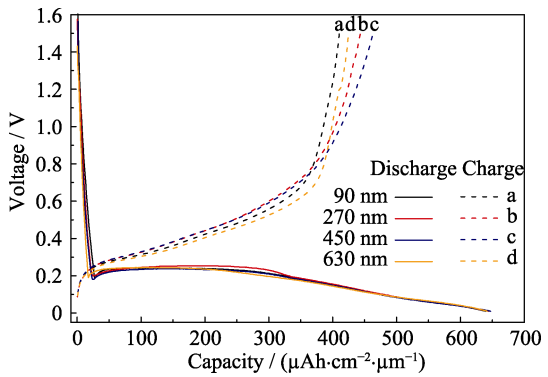

Fig. 2　The 1st cycle charge-discharge curves of $SiO_{0.7}$ film electrodes with different thickness of 90 nm, 270 nm, 450 nm and 630 nm

compounds like Li_2O and Li_4SiO_4 during the first few cycles is another important consideration causing the low ICE in SiO_x anodes[16,18,24].

The Li^+ insertion/extraction reactions between Li and SiO_x film species were studied by cyclic voltammetry (CV). Fig. 3 shows the initial five CV scans of the $SiO_{0.7}$ film electrodes with a thickness of 90 nm (Fig. 3(a)) and 450 nm (Fig. 3(b)). In the first scanning cycle, there is a cathodic peak around 0.5 V, which disappears in the following cycles, indicating a nonreversible reaction (Fig. S1(b)). The reduction peak is associated with the formation of a stable solid electrolyte interphase (SEI) passivation layer on the surface of the $SiO_{0.7}$ film[25], which is the reason for low initial Coulombic efficiency (Fig. 2). In both 90 nm and 450 nm electrodes, four redox peaks are observed in all five cyclic voltammograms, including two cathodic peaks at 0.21 V and 0.08 V, and two anodic peaks at 0.45 V and 0.29 V. They are attributed to the electrochemical reaction of lithium ions insertion and extraction in $SiO_{0.7}$ films[26]. It is observed that the four redox peaks are almost overlapped and little shift in the five cycles, indicating that an excellent cycling performance and a small polarization of the electrode.

Fig. 4(a) shows the cycle performance of $SiO_{0.7}$

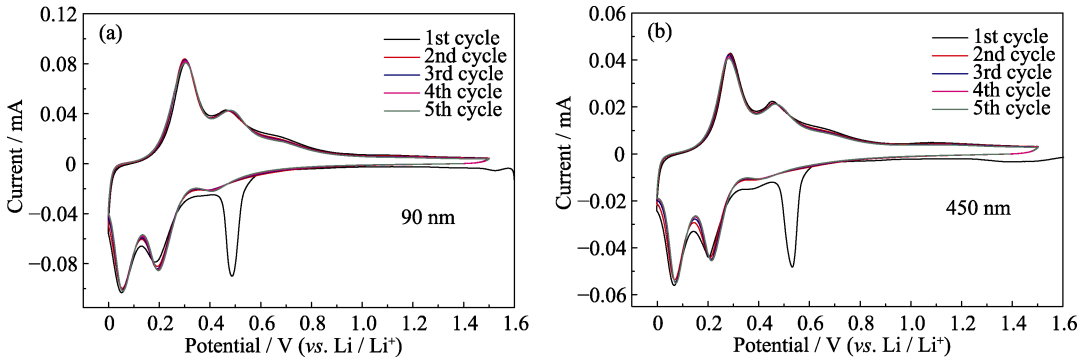

Fig. 3 Cyclic voltammograms of $SiO_{0.7}$ film electrode with thickness of (a) 90 nm and (b) 450 nm of the 1st, 2nd, 3rd, 4th and 5th cycle at a scan rate of 0.05 $mV \cdot s^{-1}$ in the potential range of 0.01 V-1.5 V

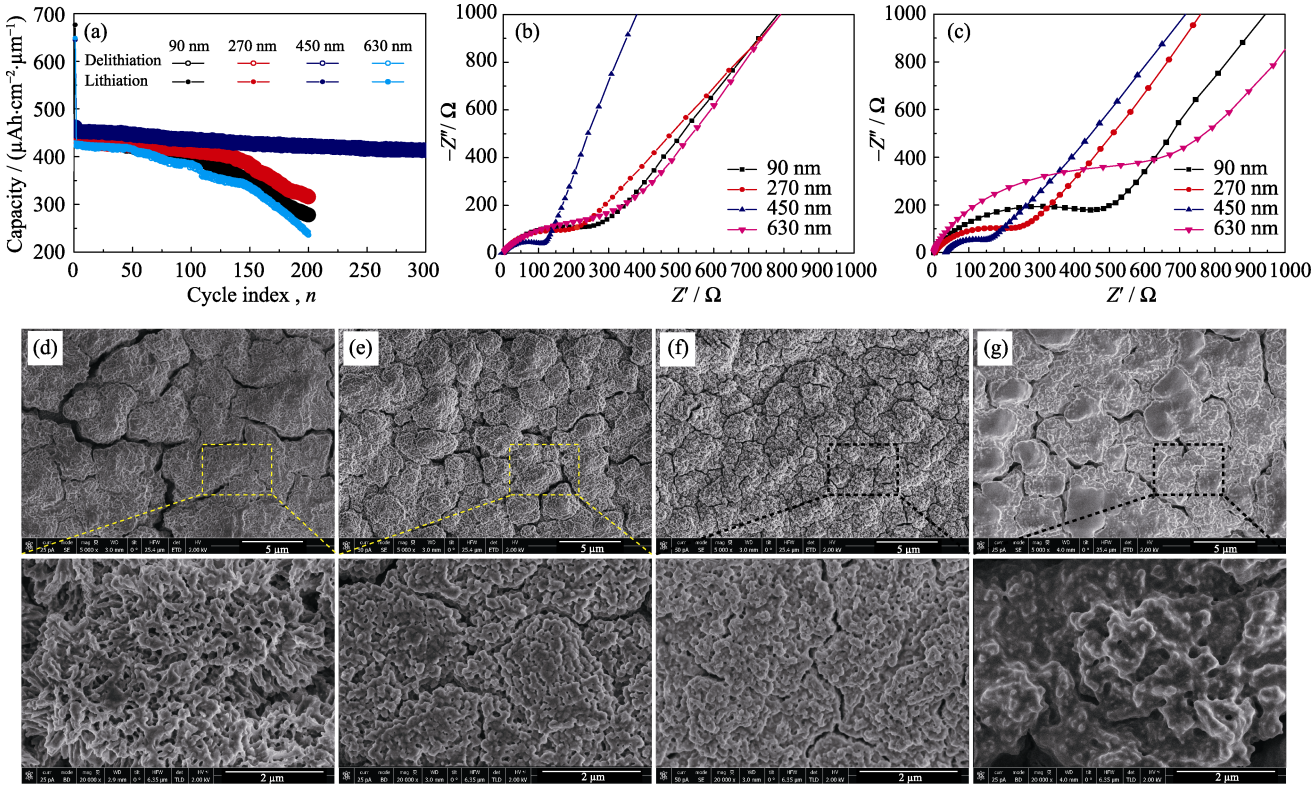

Fig. 4 Electrochemical performances of $SiO_{0.7}$ film anodes with different thickness

(a) Cycle performance of $SiO_{0.7}$ thin film anodes with different thickness at the current density of 0.2*C*; (b,c) The Nyquist plots of the $SiO_{0.7}$ thin film anodes with different thickness after (b) the 1st cycle and (c) the 200th cycle; (d-g) Surface morphologies of the 200th-cycled $SiO_{0.7}$ thin film anodes with thickness of 90 nm, 270 nm, 450 nm, and 630 nm

anodes with various film thickness. It can be seen that there exists an optimum thickness in terms of $SiO_{0.7}$ anodes[27]. As the thickness increases from 90 nm to 270 nm, 450 nm and then 630 nm, the $SiO_{0.7}$ based anodes deliver a discharge/charge capacity of 675.4/433.8, 647.4/445.1, 644.7/462.1 and 648.3/428.8 $\mu Ah \cdot cm^{-2} \cdot \mu m^{-1}$, leading to a corresponding ICE of 64.23%, 68.75%, 71.68% and 66.14%. After 200 cycles, the discharge capacities for these electrodes are 286.0 $\mu Ah \cdot cm^{-2} \cdot \mu m^{-1}$, 321.4 $\mu Ah \cdot cm^{-2} \cdot \mu m^{-1}$, 425.2 and 242.9 $\mu Ah \cdot cm^{-2} \cdot \mu m^{-1}$, corresponding to a capacity retention of 64.43%, 72.20%, 92.01% and 56.65%. These results demonstrate that the $SiO_{0.7}$ of a specified thickness of 450 nm shows the excellent cycle performance with the high capacity. The good cyclability of $SiO_{0.7}$ anode with a thickness of 450 nm is also observed from the overlapped voltage profiles (Fig. S1).

To understand such a relationship between thickness and electrochemical performance, the EIS after cycling for 200 cycles were collected (Fig. 4(b)–(c)). After the 1st cycle, the charge-transfer resistance (R_{ct}) of $SiO_{0.7}$ anodes with the specified thickness of 90 nm, 270 nm, 450 nm and 630 nm are fitted to be 173 $\Omega \cdot cm^2$, 110 $\Omega \cdot cm^2$, 86 $\Omega \cdot cm^2$ and 141 $\Omega \cdot cm^2$, respectively. These impedances increase to 322 $\Omega \cdot cm^2$, 149 $\Omega \cdot cm^2$, 94 $\Omega \cdot cm^2$ and 345 $\Omega \cdot cm^2$ after the 200th cycle. The $SiO_{0.7}$ anode with a thickness of 450 nm demonstrates the minimum R_{ct} as well as the variation during cycling. Such a low resistance should be a synergy effect between the rough Cu substrate, the moderate thickness of SEI layer and the suitable amounts of the inactive lithium compounds formed during discharge. The surface morphologies of SiO_x anodes after the 200th cycle are shown in Fig. 4(d)-(g). First of all, all the dense SiO_x films change into porous aggregates consisting of interconnected particles in the size of hundred nanometers. The porosity decreases with increasing film thickness. If more porous, the contact area between the electrodes and the electrolytes increases, enhancing formation of the SEI layers. Between the porosity and the SEI layer formed on porous electrode surfaces, the $SiO_{0.7}$ anode with a thickness of 450 nm should be the balance that enables the decreased charge transfer resistance. Second, many cracks appear in all the SiO_x films. The $SiO_{0.7}$ anode in thickness of 450 nm suffers less than the other three samples, endowing the interconnected paths for lithium transport inside the electrodes.

3 Conclusions

By means of thin-film type electrodes, the role of film thickness playing in the performance of SiO_x anodes was investigated. It is found that changing the film thickness (90 nm–450 nm) of $SiO_{0.7}$ dramatically influences the cycle stability, initial Coulombic efficiency and reversible capacity. The $SiO_{0.7}$ anode with a thickness of 450 nm exhibits the superior performance in terms of cyclability, capacity and ICE. The highest initial Coulombic efficiency (ICE) is 71.68% and the highest capacity retention is 92.01%. This benefits from the low charge transfer resistance, reduced formation of SEI layer and improved electrode integrity upon cycling, as evidenced by SEM images and EIS. All these benefits should stem from the moderate thickness of $SiO_{0.7}$ film anode, which induces the synergistic effect on formation of such insulators like lithium oxide/silicates during discharge. Functions such configuration as physical buffers, which relieve the large volume change of *in situ* formed Si particles from the reduction of SiO_x, and shield the electrolytes from further decomposition by suppressing electron leakage on the electrode surfaces. These results suggest that the control of the film thickness of SiO_x is the key factor to improve the eletrochemical performance.

References

[1] HATCHARD T D, DAHN J R. *In situ* XRD and electrochemical study of the reaction of lithium with amorphous silicon. *Journal of the Electrochemical Society*, 2004, **151(6):** A838–A842.

[2] GAO T, QU Q, ZHU G, *et al*. A self-supported carbon nanofiber paper/sulfur anode with high-capacity and high-power for application in Li-ion batteries. *Carbon*, 2016, **110:** 249–256.

[3] MA H, JIANG H, JIN Y, *et al*. Carbon nanocages@ultrathin carbon nanosheets: one-step facile synthesis and application as anode material for lithium-ion batteries. *Carbon*, 2016, **105:** 586–592.

[4] CHAN C K, PENG H L, LIU G, *et al*. Crystalline-amorphous core-shell silicon nanowires for high capacity and high current battery electrodes. *Nature Nanotechnology*, 2008, **3:** 31–35.

[5] YANG H, FAN F, LIANG W, *et al*. A chemo-mechanical model of lithiation in silicon. *Journal of the Mechanics & Physics of Solids*, 2014, **70(1):** 349–361.

[6] KIM H, CHO J. Superior lithium electroactive mesoporous Si@carbon core-shell nanowires for lithium battery anode material. *Nano Letters*, 2008, **8(11):** 3688–3691.

[7] PENG K, JIE J, ZHANG W, *et al*. Silicon nanowires for rechargeable lithium-ion battery anodes. *Applied Physics Letters*, 2008, **93(3):** 033105–1–3.

[8] MIYAZAKI R, OHTA N, OHNISHI T, *et al*. Anode properties of silicon-rich amorphous silicon suboxide films in all-solid-state lithium batteries. *Journal of Power Sources*, 2016, **329:** 41–49.

[9] TAKEZAWA H, IWAMOTO K, ITO S, *et al*. Electrochemical behaviors of nonstoichiometric silicon suboxides (SiO_x) film prepared by reactive evaporation for lithium rechargeable batteries. *Journal of Power Sources*, 2013, **244:** 149–157.

[10] SONG S W. Roles of oxygen and interfacial stabilization in enhancing the cycling ability of silicon oxide anodes for rechargeable lithium batteries. *Journal of the Electrochemical Society*, 2013, **160(6):** A906–A914.

[11] MARIKO M, HIRONORI Y, HIDEMASA K, *et al*. Analysis of SiO anodes for lithium-ion batteries. *Journal of the Electrochemical Society*, 2005, **152(10):** 4803–4837.
[12] ZHAO J, LEE H W, SUN J, *et al*. Metallurgically lithiated SiO_x anode with high capacity and ambient air compatibility. *Proceedings of the National Academy of Sciences of the United States of America*, 2016, **113(27):** 7408–7413.
[13] HIRATA A, KOHARA S, ASADA T, *et al*. Atomic-scale disproportionation in amorphous silicon monoxide. *Nature Communications*, 2016, **7:** 11591–1–7.
[14] XU Q, SUN J K, YIN Y X, *et al*. Facile synthesis of blocky SiO_x/C with graphite-like structure for high-performance lithium-ion battery anodes. *Advanced Functional Materials*, 2018, **28(8):** 1705235–1–7.
[15] LEE J I, CHOI N S, PARK S. Highly stable Si-based multi-component anodes for practical use in lithium-ion batteries. *Energy & Environmental Science*, 2012, **5(7):** 7878–7882.
[16] CUI Z, GUO X, LI H. Improved electrochemical properties of MnO thin film anodes by elevated deposition temperatures: study of conversion reactions. *Electrochimica Acta*, 2013, **89:** 229–238.
[17] CUI Z, GUO X, LI H. High performance MnO thin-film anodes grown by radio-frequency sputtering for lithium ion batteries. *Journal of Power Sources*, 2013, **244(4):** 731–735.
[18] BARANCHUGOV V, MARKEVICH E, POLLAK E, *et al*. Amorphous silicon thin films as a high capacity anodes for Li-ion batteries in ionic liquid electrolytes. *Electrochemistry Communications*, 2007, **9(4):** 796–800.
[19] BUSTARRET E, HACHICHA M A, BRUNEL M. Experimental determination of the nanocrystalline volume fraction in silicon thin films from Raman spectroscopy. *Applied Physics Letters*, 1988, **52(20):** 1675–1677.
[20] CHEN T, WU J, ZHANG Q, *et al*. Recent advancement of SiO_x based anodes for lithium-ion batteries. *Journal of Power Sources*, 2017, **363:** 126–144.
[21] BELL F G, LEY L. Photoemission study of SiO_x ($0 \leqslant x \leqslant 2$) alloys. *Physical Review B: Condensed Matter*, 1988, **37(14):** 8383–8393.
[22] VAN HAPERT J J, VREDENBERG A M, VAN FAASSEN E E, *et al*. Role of spinodal decomposition in the structure of SiO_x. *Physical Review B: Condensed Matter*, 2004, **69(24):** 1681–1685.
[23] HANG Q, PAN J, LU P, *et al*. Synergetic effects of inorganic components in solid electrolyte interphase on high cycle efficiency of lithium ion batteries. *Nano Letters*, 2016, **16(3):** 2011–2016.
[24] CHEN T, WU J, ZHANG Q, *et al*. Recent advancement of SiO_x based anodes for lithium-ion batteries. *Journal of Power Sources*, 2017, **363:** 126–144.
[25] CHEN L B, XIE J Y, YU H C, *et al*. An amorphous Si thin film anode with high capacity and long cycling life for lithium ion batteries. *Journal of Applied Electrochemistry*, 2009, **39(8):** 1157–1162.
[26] HUO H Y, SUN J Y, CHENG C, *et al*. Flexible interfaces between Si anodes and composite electrolytes consisting of poly (propylene carbonates) and garnets for solid-state batteries. *Journal of Power Sources*, 2018, **383:** 150–156.
[27] SHI S Q, GAO J, LIU Y, *et al*. Multi-scale computation methods: their applications in lithium-ion battery research and development. *Chinese Physics B*, 2016, **25(1):** 174–197.

薄膜厚度对 α-SiO_x 薄膜负极电化学性能的影响

孟祥鲁[1,2,3], 霍翰宇[1,2], 郭向欣[1,4], 董绍明[1]

(1. 中国科学院 上海硅酸盐研究所, 高性能陶瓷和超微结构国家重点实验室, 上海 200050; 2. 中国科学院大学, 北京 100049; 3. 上海科技大学 物质科学与技术学院, 上海 201210; 4. 青岛大学 物理学院, 青岛 266071)

摘 要: 近年来, SiO_x 作为锂离子电池负极, 由于其良好的循环稳定性、较大的容量以及对成分调控的可行性, 引起了广泛的关注。以往的许多研究都集中在阐明氧含量对 SiO_x 负极的影响, 尺寸效应对性能的影响规律很少被研究。此工作研究了不同厚度的薄膜型 SiO_x 负极材料的电化学性能。溅射制备 SiO_x 电极的 Si/O 比值为 0.7、膜厚为 450 nm 时, 电极初始库仑效率(ICE)为 71.68%、容量保持率 92.01%。以上的最优性能主要归功于电荷转移电阻低、SEI 层形成减少和循环过程中电极的结构稳定性。研究表明, 作为 LIBs 负极, 控制 SiO_x 负极的厚度可以有效改善电极材料的电化学性能。

关 键 词: SiO_x 薄膜负极; 薄膜厚度; 循环稳定性; 容量; 锂离子电池

中图分类号: TQ174 **文献标识码:** A

Supporting information

Influence of Film Thickness on the Electrochemical Performance of α-SiO_x Thin-film Anodes

MENG Xiang-Lu[1,2,3], HUO Han-Yu[1,2], GUO Xiang-Xin[1,4], DONG Shao-Ming[1]

(1. State Key Laboratory of High Performance Ceramics and Superfine Microstructure, Shanghai Institute of Ceramics, Chinese Academy of Sciences, Shanghai 200050, China; 2. University of Chinese Academy of Sciences, Beijing 100049, China; 3. College of Material Science and Technology, ShanghaiTech University, Shanghai 201210, China; 4. College of Physics, Qingdao University, Qingdao 266071, China)

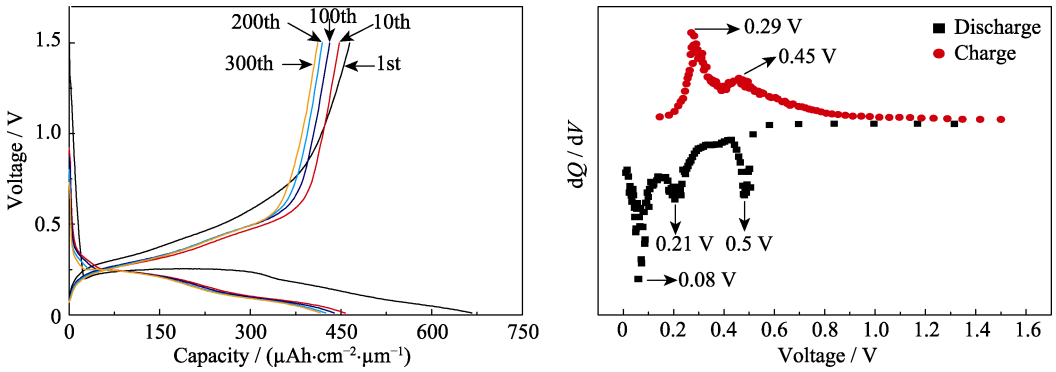

Fig. S1　(a) The galvanostatic discharge-charge voltage profiles of the $SiO_{0.7}$ anodes with a thickness of 450 nm of 1st, 10th, 100th, 200th and 300th cycle and (b) the dQ/dV differential curve of the first cycle profile of the $SiO_{0.7}$ anodes with a thickness of 450 nm